Lecture 6 — Scattering geometries.

1 Cross section for a "small" perfect single crystal

Our goal in this section is to calculate the scattering cross section from a "small" single crystal. As with many things in physics, the idea of a "small" crystal is a somewhat inconsistent abstraction, because the derivation implies that the crystal be still large enough to be considered "infinite", but be small enough to ignore mulitple scattering events (see extended lecture notes for a fuller discussion). For the sake of argument, we will treat the case of X-rays, although, as we shall see, the other cases (neutrons, electron beams) yield very similar results. Using the far-field approximation, we can develop exactly the same argument we used to calculate the form factors, but, this time, we extend the volume integral to the *whole crystal*. Following the same procedure explained in the previous lecture, the scattering amplitude becomes:

$$\boxed{A(\mathbf{q}) = r_0 \int_{Crystal} d\mathbf{R} f(\mathbf{R}) e^{-i\mathbf{q}\cdot\mathbf{R}} \left[\boldsymbol{\epsilon}\cdot\boldsymbol{\epsilon}'\right]} \tag{1}$$

We can exploit the fact that the charge density is periodic, so that, if $\mathbf{R}_i$ is a lattice translation and $\mathbf{r}$ is restricted to the unit cell containing the origin:

$$f(\mathbf{R}) = f(\mathbf{R}_i + \mathbf{r}) = f(\mathbf{r}) \tag{2}$$

whence the scattering amplitude becomes

$$\begin{aligned} A(\mathbf{q}) &= r_0 \sum_i \int_{Unit\,Cell} d\mathbf{r} f(\mathbf{r}) e^{-i\mathbf{q}\cdot(\mathbf{R}_i+\mathbf{r})} \left[\boldsymbol{\epsilon}\cdot\boldsymbol{\epsilon}'\right] \\ &= r_0 \sum_i e^{-i\mathbf{q}\cdot\mathbf{R}_i} \int_{Unit\,Cell} d\mathbf{r} f(\mathbf{r}) e^{-i\mathbf{q}\cdot\mathbf{r}} \left[\boldsymbol{\epsilon}\cdot\boldsymbol{\epsilon}'\right] \end{aligned} \tag{3}$$

where the summation runs over all the unit cells in the crystal. The expression

$$\boxed{F(\mathbf{q}) = r_0 \int_{Unit\,Cell} d\mathbf{r} f(\mathbf{r}) e^{-i\mathbf{q}\cdot\mathbf{r}}} \tag{4}$$

is known as the **structure factor**.

The structure factor is proportional to the Fourier transform of the charge density (or, more in general, scattering density) integrated over the unit cell.

If the electron density $f(\mathbf{r})$ is a superposition of atomic-like electron densities, it is easy to show that $F(\mathbf{q})$ can be written as

$$F(\mathbf{q}) = r_0 \sum_n f_n(\mathbf{q}) e^{-i\mathbf{q}\cdot\mathbf{r}_n} \tag{5}$$

where the sum runs over all the atoms in the unit cell and $f_n(\mathbf{q})$ are the form factors of each species and $\mathbf{r}_n$ are their positions within the unit cell.

We can now calculate the cross section:

$$\frac{d\sigma}{d\Omega} = A(\mathbf{q})A^*(\mathbf{q}) = \left(\sum_j \sum_i e^{-i\mathbf{q}\cdot(\mathbf{R}_i - \mathbf{R}_j)} \right) |F(\mathbf{q})|^2 \left[\boldsymbol{\epsilon}\cdot\boldsymbol{\epsilon}'\right]^2 \tag{6}$$

We now introduce the fact that the double summation in parentheses can be consider as running over an infinite lattice. Consequently, all the summations over i labelled by $\mathbf{r}_j$ are the same (they only differ by a shift in origin), and the summation over j can be replaced by multiplication by N_c — the number of unit cells in the crystal ($\to \infty$).

As we have already remarked, the remaining single summation is only non-zero when $\mathbf{q}$ is a RL vector. If $\mathbf{q}$ is restricted to the first Brillouin zone, we can write:

$$\delta(\mathbf{q}) = \frac{1}{(2\pi)^3} \int d\mathbf{x} e^{-i\mathbf{q}\cdot\mathbf{x}} \simeq \frac{v_0}{(2\pi)^3} \sum_i e^{-i\mathbf{q}\cdot\mathbf{R}_i} \tag{7}$$

where v_0 is the unit cell volume. For an unrestricted $\mathbf{q}$, the same expression holds with the left-hand member replaced by a sum of delta functions centred at all reciprocal lattice nodes, indicated with $\boldsymbol{\tau}$ in the remainder. With this, we can write the final expression for the cross section:

$$\frac{d\sigma}{d\Omega} = N_c \frac{(2\pi)^3}{v_0} \sum_{\boldsymbol{\tau}} \delta(\mathbf{q} - \boldsymbol{\tau}) |F(\boldsymbol{\tau})|^2 \left[\boldsymbol{\epsilon}\cdot\boldsymbol{\epsilon}'\right]^2 \tag{8}$$

As in the case of the scattering from a single electron or atom, the term $\left[\boldsymbol{\epsilon}\cdot\boldsymbol{\epsilon}'\right]^2$ needs to be averaged over all this incident and scattered polarisations, yielding a **polarisation factor** $\mathcal{P}(\gamma)$,

which depends on the experimental setting. For example, for an unpolarised incident beam and no polarisation analysis:

$$\boxed{\mathcal{P}(\gamma) = \left[\frac{1+\cos^2\gamma}{2}\right] \quad \textbf{unpolarised beam}} \tag{9}$$

The final general expression for the average cross section is:

$$\boxed{\frac{d\sigma}{d\Omega} = N_c \frac{(2\pi)^3}{v_0} \sum_{\boldsymbol{\tau}} \delta(\mathbf{q}-\boldsymbol{\tau}) |F(\boldsymbol{\tau})|^2 \mathcal{P}(\gamma)} \tag{10}$$

Let's recap the key points to remember:

- **The cross section is proportional to the number of unit cells in the crystal. The bigger the crystal, the more photons or particles will be scattered. We can clearly see that this result *must* involve an approximation: the scattered intensity must reach a limit when all the particles in the beam are scattered.**
- **The cross section is proportional to the squared modulus of the structure factor (no surprises here — you should have learned this last year).**
- **Scattering only occurs at the nodes of the RL. For a perfect, infinite crystal, this is in the form of delta functions.**
- **The cross section contains the unit-cell volume in the denominator. This is necessary for dimensional reasons, but it could perhaps cause surprise. After all, we could arbitrarily decide to *double* the size of the unit cell by introducing a "basis". The answer is, naturally, that the $|F(\boldsymbol{\tau})|^2$ term exactly compensates for this.**

2 The effect of atomic vibrations — the Debye-Waller factor

2.1 D-W factors — qualitative discussion

Up to this point, we have explicitly assumed perfect periodicity — in other words, that the electron densities of all the unit cells are identical, or, for atomic-like electron densities, that the atoms are in identical positions in all unit cells. This is, of course, never the case. Atoms are

always displaced away from their "ideal" positions, primarily due to thermal vibrations, but also due to crystal defects. We now want to examine the effect of these displacements and relax the perfect periodicity condition. Let us re-write the expression of the scattering amplitude (eq. 3), adapted to the atomic case (we omit the polarisation factor $[\boldsymbol{\epsilon} \cdot \boldsymbol{\epsilon}']$ for simplicity):

$$A(\mathbf{q}) = r_0 \sum_i e^{-i\mathbf{q}\cdot\mathbf{R}_i} \sum_n f_n(\mathbf{q}) e^{-i\mathbf{q}\cdot(\mathbf{r}_n + \mathbf{u}_{n,i})} \tag{11}$$

where $\mathbf{u}_{n,i}$ is the *displacement vector* characterising the position of the atom with label n in the i^{th} unit cell.

Bragg scattering results from **time averaging of the scattering *amplitude*** (*not* the cross section — for a somewhat hand-waving justification, see the extended version of the notes). The effect of this is that

Atomic vibrations "smear out" the scattering density, acting, in a sense as an additional "form factor".

- **The higher the temperature, the more the atoms will vibrate, the more the intensity will decay at high q. This is easily understood by analogy with the form factor $f(\mathrm{q})$: the more the atoms vibrate, the more "spread" out the scattering density will be, the faster the scattering will decay at high q.**
- **The *softer* the spring constants, the more the atoms will vibrate, the more the intensity will decay at high q.**
- **The *lighter* the atoms, the more the atoms will vibrate, the more the intensity will decay at high q.**

2.2 D-W factors — functional form

Being content with this qualitative discussion for the moment, we can re-write eq. 11 as

$$A(\mathbf{q}) = r_0 \sum_i e^{-i\mathbf{q}\cdot\mathbf{R}_i} \sum_n f_n(\mathbf{q}) e^{-i\mathbf{q}\cdot\mathbf{r}_n} \left\langle e^{-i\mathbf{q}\cdot\mathbf{u}_{n,i}} \right\rangle \tag{12}$$

where $\langle\rangle$ indicates time averaging. Needless to say that the expression in $\langle\rangle$ *does not depend on i*, since, once the averaging is performed, the position of the unit cell in the crystal is immaterial (they will all average to identical values). We already see from here that *the effect of thermal vibrations can be incorporated in the structure factor*. To complete our derivation, we need one

more step, known as the **Bloch's identity**, which is valid in the harmonic approximation. We will just state the result here:

$$\left\langle e^{-i\mathbf{q}\cdot\mathbf{u}_{n,i}} \right\rangle = e^{\frac{1}{2}\left\langle (-i\mathbf{q}\cdot\mathbf{u}_n)^2 \right\rangle} = e^{-\frac{1}{2}\left\langle (\mathbf{q}\cdot\mathbf{u}_n)^2 \right\rangle} = e^{-W(\mathbf{q},n)}. \tag{13}$$

W is a positive-definite quantity, known as the **Debye-Waller factor**. It is also a *quadratic function of* $\mathbf{q}$, so its most general expression is

$$W(\mathbf{q}, n) = U^{ij}(n) q_i q_j = \mathbf{q}\overline{\overline{\mathbf{U}}}_n\mathbf{q} \tag{14}$$

where $U^{ij}(n)$ is, in general, a *tensor*.

Here, n labels the specific atomic site.

2.2.1 Isotropic case

Keeping in mind that atoms usually vibrate with different amplitudes in different directions (anisotropic case), we will only treat hear the simplest case. When all atoms vibrate with the same amplitude in all directions **isotropic case**, $U^{ij}(n)$ is proportional to the unit matrix and

$$\boxed{W(\mathbf{q}, n) = U_n\, q^2} \tag{15}$$

With this, we obtain the **general expression for the X-ray structure factor in the isotropic case**

$$\boxed{F(\mathbf{q}) = r_0 \textstyle\sum_n f_n(q) e^{-i\mathbf{q}\cdot\mathbf{r}_n} e^{-U_n\, q^2}} \tag{16}$$

A very similar expression is found for the ***coherent*** **neutron structure factors for nuclear scattering**.

$$\boxed{F(\mathbf{q}) = \textstyle\sum_n b_n e^{-i\mathbf{q}\cdot\mathbf{r}_n} e^{-U_n\, q^2}} \tag{17}$$

The corresponding formula for **magnetic scattering of neutrons from a collinear ferromagnet or antiferromagnet** is

$$\boxed{F(\mathbf{q}) = \gamma_N r_0 \sum_n f_n(\boldsymbol{q}) M_n \sin\alpha(\mathbf{q}) \mathbf{e}^{-\mathbf{i q \cdot r_n}} \mathbf{e}^{-\mathbf{U_n q^2}}} \tag{18}$$

where M_n (expressed in Bohr magnetons) reflects both the magnitude and the sign of the magnetic moment of atom n, and $fm_n(\boldsymbol{q})$ is the corresponding magnetic form factor and α is the angle between $\mathbf{M}$ and $\mathbf{q}$

3 Laue and Bragg equations

The δ function in eq. 8 implicitly contains the geometrical conditions for observing scattering from a single crystal, which are traditionally named **Laue equations** [1]:

$$\mathbf{q} = h\mathbf{a}^* + k\mathbf{b}^* + l\mathbf{c}^* \tag{19}$$

$$\begin{aligned} \mathbf{q} \cdot \mathbf{a}_1 &= (\mathbf{k}_f - \mathbf{k}_i) \cdot \mathbf{a}_1 = 2\pi h \\ \mathbf{q} \cdot \mathbf{a}_2 &= (\mathbf{k}_f - \mathbf{k}_i) \cdot \mathbf{a}_2 = 2\pi k \\ \mathbf{q} \cdot \mathbf{a}_3 &= (\mathbf{k}_f - \mathbf{k}_i) \cdot \mathbf{a}_3 = 2\pi l \end{aligned} \tag{20}$$

where h, k and l are the **Miller indices** that we have already encountered.

The Laue equations are nothing but a re-statement of the fact that *q* must be a RL vector

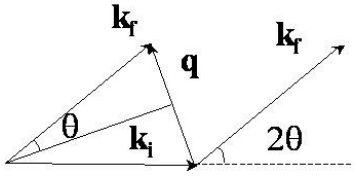

Figure 1: Scattering triangle for elastic scattering.

A second important relation can be obtained by considering the *modulus* of the scattering vector, for which, as we have already seen (fig. 1 and eq. 21 are reproduced here for convenience):

[1] Throughout this part of the course, we will employ the convention that $\boldsymbol{q}$ is *the change of wavevector of the particle or photon*, so $\boldsymbol{q} = \boldsymbol{k}_f - \boldsymbol{k}_i$. the convention $\boldsymbol{q} = \boldsymbol{k}_i - \boldsymbol{k}_f$ identifies $\boldsymbol{q}$ with the wavevector *transferred to the crystal*, and is widely employed particularly in the context of inelastic scattering

$$q = |\mathbf{q}| = \frac{4\pi \sin\theta}{\lambda} \tag{21}$$

The quantity

$$\boxed{d = \frac{2\pi}{q}} \tag{22}$$

is known as the **d-spacing**. From eqs. 21 and 22 we obtain the **familiar formulation of Bragg's law**:

$$\boxed{2d \sin\theta = \lambda} \tag{23}$$

The d-spacing can be identified with the spacing between families of lattice planes *perpendicular* to a given RL vector.

4 Geometries for diffraction experiments

In general terms, the experimental apparatus to perform a diffraction experiment on a single crystal or a collection of small crystals (powder diffraction) will consist of

- An **incident beam**, which can be **monochromatic** or **polychromatic**. The **divergence** of the incident beam is of course an important parameter, in that it determines the uncertainty on the Bragg angle 2θ. Various focussing schemes are possible to increase the flux on the sample or at the detector position whilst limiting the loss of resolution.
- A **sample stage**, which enables the sample to be oriented (typically a simple uniaxial rotator for powder diffraction, a Eulerian cradle or analogous arrangements for single crystal experiments). The sample stage also incorporates the **sample environment** to control a variety of physical (P, T, H...) and/or chemical parameters.
- A **detector**, which includes a detector of photons or particles. Many technologies are available (gas tube, scintillator, CCD, solid-state...), depending on the type of radiation, detector coverage and resolution required. This is normally mounted on a separate arm, enabling the 2θ angular range to be varied. On the detector arm, one often finds other devices, such as

as **analyser crystal** and/or **receiving slits** to define the angular divergence of the scattered beam and, in the case of the analyser, to reject parasite radiation due to fluorescence.

In this section, we will focus on two among the most important important geometries for diffraction experiments: the **single-crystal 4-circle diffractometer** and the **Debye-Scherrer powder diffractometer**. Several other geometries are described in the extended version of these notes. In their simplest form, both these geometries employ a **point detector**, with a spatial resolution defined by a set of vertical and horizontal slits. Early diffractometers made extensive use of **photographic film**. Modern single-crystal and powder diffractometers generally employ a **pixillated area detector**. As an introduction to each method, we will describe two important geometrical constructions: the **Ewald construction** (most useful for single-crystal experiments) and the **Debye-Scherrer construction** (for powder diffraction).

4.1 Single-crystal diffraction

4.1.1 Scattering triangles for elastic scattering and the Ewald construction

As we have seen, the scattering cross section for a single crystal is a series of delta functions in reciprocal space, centred at the nodes of the reciprocal lattice. When a single crystal is illuminated with monochromatic radiation, the scattering conditions are satisfied only for particular orientations of the crystal itself — in essence, the specular (mirror-like) reflection from a family of lattice planes must satisfy Bragg law at the given wavelength.

With monochromatic radiation, for a generic crystal orientation, no Bragg scattering will be observed at all.

Fig. 2 show the geometrical construction used to establish when the scattering conditions are satisfied. Note that here we employ the **diffraction convention**: $\mathbf{q} = \mathbf{k_f} - \mathbf{k_i}$. A typical problem will state the wavelength λ of the incident and scattered radiation (which are the same, since the scattering is elastic), the symmetry and the lattice parameters of the material and the Bragg reflection to be measured (given in terms of the Miller indices hkl). These data are sufficient to determine $k_i = k_f = 2\pi/\lambda$ and q (for a right-angle lattice $q = 2\pi\sqrt{h^2/a^2 + k^2/b^2 + l^2/c^2}$). Since all the sides of the scattering triangle are known, it is possible to determine all the angles — in particular the scattering angle $\gamma = 2\theta$ and the orientation of the incident beam with respect to the lattice required to be in scattering condition.

The circle shown in fig. 2 is actually a sphere in 3D, and defines the *locus* of all the possible scattering vectors for a given $\mathbf{k_i}$. This is known as the **Ewald sphere**, from the German physicist Paul Peter Ewald (1888, 1985).

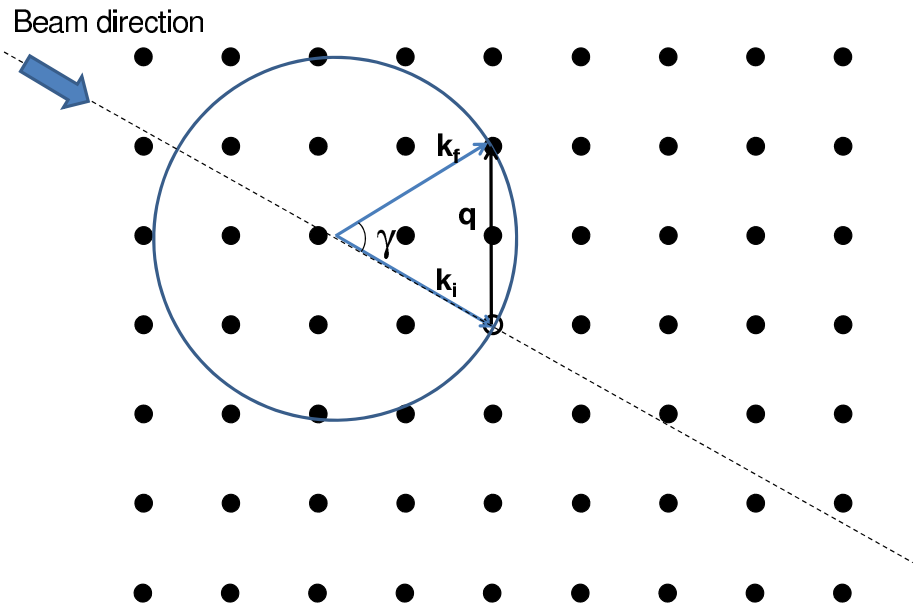

Figure 2: The procedure to construct the scattering triangle for elastic scattering.

4.1.2 Four-circle diffractometry

For single-crystal experiments with monochromatic radiation, it is quite apparent that one should strive to maintain the maximum flexibility in orienting the crystal. One way to accomplish this is to mount the crystal in an *Eulerian cradle*, as illustrated in fig. 3 (note the alternative nomenclature for the angles). The whole assembly, including the detector arm, is known as a **four-circle diffractometer**. With a four-circle diffractometer, one can in principle (barring mechanical collisions and shadowing effects) access all nodes of the reciprocal space that are accessible for a given wavelengh. It can be shown (left as an exercise) that the nodes "accessible" by scattering are contained within a sphere of radius $2k_i = 4\pi/\lambda$, centered on the origin of reciprocal space, so that

$$0 \leq q \leq k_i = k_f \tag{24}$$

This is equivalent to saying that **the shortest accessible d-spacing is 1/2 the wavelength** — a statement that can be easily verified from Bragg law by setting θ to have its maximum value (90° in backscattering; the $\lambda/2$ limit is often referred to as the **Bragg cut-off**).

Modern four-circle diffractometers often employ an alternative, more open geometry, known as κ **geometry**; here the κ-axis, which replaces the χ-axis, is not perpendicular to the Ω-axis, but forms an angle of approximately 60° with it.

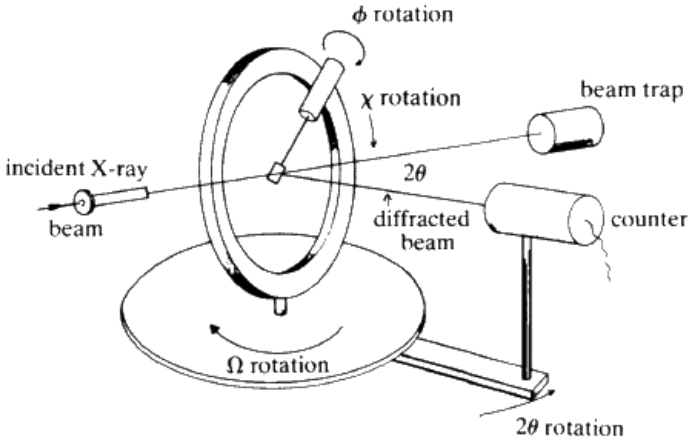

Figure 3: The geometry of a "four circle" single-crystal diffractometer. The "four circles" (actually four axes) are marked "ϕ", "χ", "Ω" and "2θ". The 2θ and Ω angles are also known as γ and η — a notation we will often employ in the remainder to avoid clutter and confusion with other symbols (e.g., the solid angle)

4.1.3 Scattering triangles for inelastic scattering

Although inelastic scattering — particularly inelastic scattering of neutrons using triple-axis instruments — will be treated later on in the course, we will discuss here the purely *geometrical* aspects, since the construction of the scattering triangles is very similar to the elastic scattering case. One should note that, for inelastic scattering, the **inelastic convention**: $\mathbf{q} = \mathbf{k_i} - \mathbf{k_f}$ is generally employed, so that $\mathbf{q_{dif}} = -\mathbf{q_{ine}}$.

In an inelastic scattering experiment, the scattered particle loses (**energy loss scattering**) or gains (**energy gain scattering**) part of its energy, and a corresponding amount of energy is transferred to or from an excitation in the crystal such as a *phonon* or a *magnon*. In constructing the scattering triangle, we should therefore allow for the fact that k_f will be either larger or smaller than k_i.

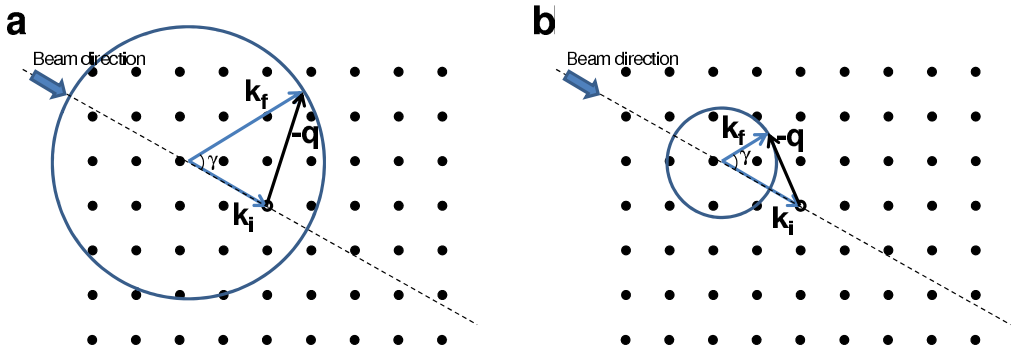

Figure 4: The procedure to construct the scattering triangle for inelastic scattering. (**a**) energy *gain*; (**b**) energy *loss*.

The corresponding constructions are shown in 4. One can see that eq. 24 should be replaced by

$$|k_i - k_f| \leq q \leq k_i + k_f \tag{25}$$

The consequence of this is the existence of a "forbidden" sphere of radius $|k_i - k_f|$ around the origin of reciprocal space.

4.2 Powder diffraction

4.2.1 Debye-Scherrer cones

A "powder" sample is a more or less "random" collection of small single crystals, known as "crystallites". **The cross section for the whole powder sample depends on the *modulus* of the scattering vector q but not on its direction**. For a monochromatic incident beam, the 2θ angle *between* the incident and scattered beam is fixed for a given Bragg reflection, but, as we just said, the angle *around* the incident beam is arbitrary. It is easy to understand that the *locus* of all the possible scattered beams is a **cone** around the direction of the incident beam.

For monochromatic powder diffraction, the scattered beams form a series of cones (fig. 5), known as Debye-Scherrer cones (D-S cones in the remainder), one for each "non-degenerate" (see below) node of the reciprocal lattice.

It follows naturally that all the symmetry-equivalent RL nodes, having the same q, *contribute to the same D-S cone*. This is also illustrated by the construction in fig. 6. Moreover, *accidentally degenerate* reflections, having the same q but unrelated hkl's, also contribute to the same D-S cone. This is the case for example, for reflections $[333]$ and $[115]$ in the cubic system, since $3^2 + 3^2 + 3^2 = 1^2 + 1^2 + 5^2$.

4.2.2 The Debye-Scherrer geometry

The Debye-Scherrer geometry employs a **parallel beam**, and the sample has a roughly cylindirical symmetry. The sample is contained in a tube (neutrons) or capillary (x-rays), and is uniformly illuminated by the incident beam. The detector(s) are placed on a "detection cylinder" (fig. 7, generally covering only a small portion of the cylinder, near the scattering plane. This geometry can employ many detectors simultaneously, as it is done in reactor-based neutron diffractometers, such as D20 and D2B at the ILL (see feig. 7. Fig. 8 shows a comparative example of X-ray and neutron high-resolution data collected on the same compound using variants of the the Debye-Scherrer geometry.

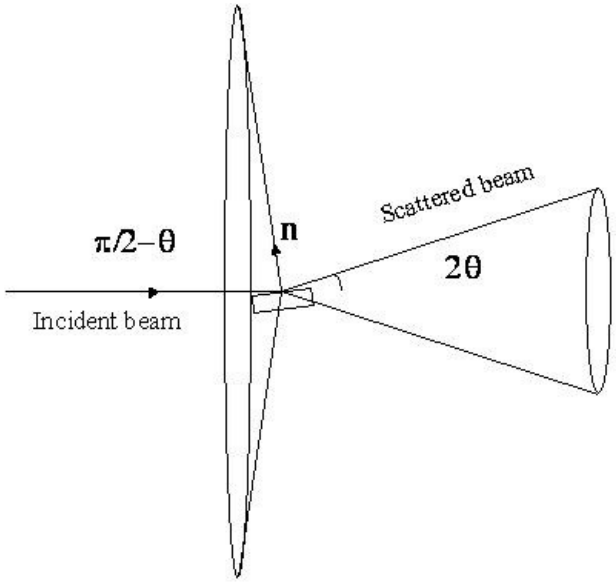

Figure 5: Debye-Scherrer cones and the orientations of the sets of Bragg planes generating them.

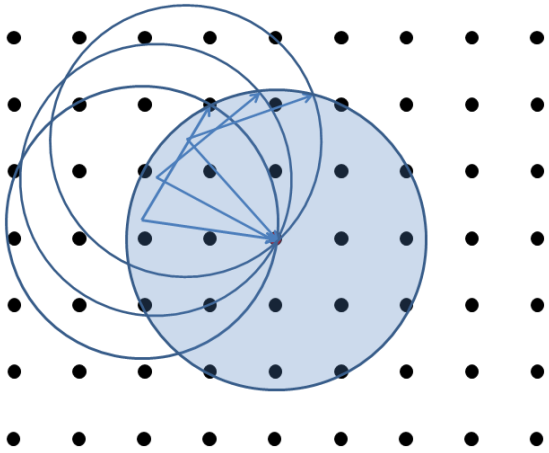

Figure 6: Ewald construction for powder diffraction, to represent the crystal being rotated randomly around the direction of the incident beam (the figure actually shows the opposite, for clarity). Note that many RL nodes are simultaneously in scattering — those that have the same $|q|$. Symmetry-equivalent reflections have the same $|q|$ and also the same structure factor. The powder intensity is therefore multiplied by the number of symmetry-equivalent reflections, known as the *multiplicity*.

Key points to retain about powder diffraction

- **In powder diffraction methods, the intensity around the D-S cones is *always integrated*, yielding a 1-dimensional pattern.**
- **Powder diffraction peaks are usually well-separated at low q, but become increasingly crowded at high q often becoming completely overlapped. This substantially reduce the amount of information available to solve or refine the structure precisely (see below).**

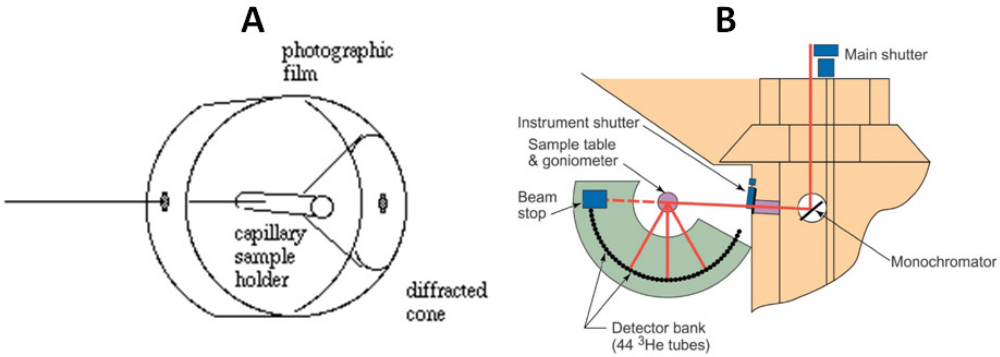

Figure 7: The Debye-Scherrer powder diffraction geometry, as implemented on a film camera (**A**) and on a modern constant-wavelength powder diffractometer (**B**). Note that, in the latter, the film has been replaced with an array of ^3He gas tubes.

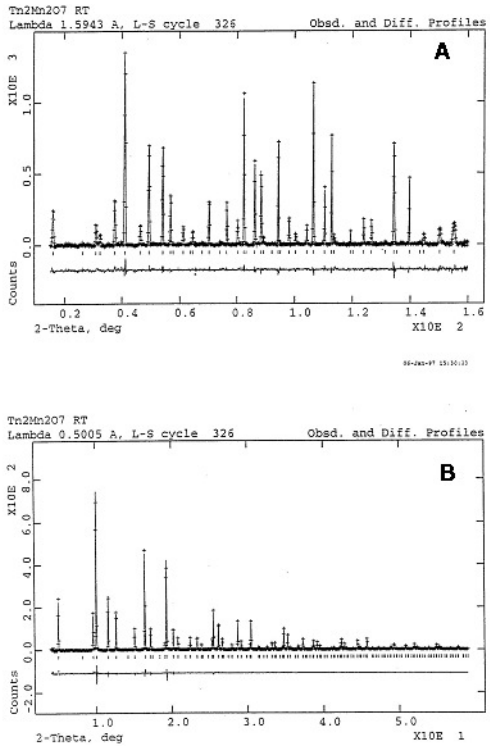

Figure 8: X-ray and neutron high-resolution powder diffraction at a glance. **A**: neutron powder diffraction (D2B-ILL, Grenoble, France, $\lambda = 1.594$) and **B** synchrotron x-ray diffraction (X7a-NSLS, Brookhaven, USA, $\lambda = 0.5000$) data on the pyrochlore compound $Tl_2Mn_2O_2$. Both data sets are fitted using the **Rietveld method** (see lecture and extended lecture notes)

Integrated intensities for dummies

Exam problems will not be concerned with profile fitting, and you will be given integrated intensities of some form. These intensities will be usually corrected for the Lorentz, polarisation, attenuation and incident flux terms, but the role these terms may be requested as part of the discussion.

The integrated intensity can always be reduced to a dimensionless quantity (counts).

- **The general expression for the integrated intensity (number of particles) is**

$$P_{\boldsymbol{\tau}} = N_c \left(\frac{d^3}{v_0}\right) m_{\boldsymbol{\tau}} \left|F(\boldsymbol{\tau})\right|^2 \mathcal{P}(\gamma)\mathcal{L}(\gamma)\mathcal{A}_{\boldsymbol{\tau}}(\lambda,\gamma)\mathcal{F}_{inc} \tag{26}$$

  - N_c **is the number of unit cells in the sample.**
  - d **is the d-spacing of the reflection.**
  - v_0 **is the unit-cell volume.**
  - $m_{\boldsymbol{\tau}}$ **(powder diffraction only) is the *number of symmetry-equivalent reflections*. This accounts for the fact that in powder diffraction these reflections are not separable, and will always contribute to the same Bragg powder peak (see previous discussion and fig. 6.**
  - $\mathcal{P}(\gamma)$ **is the *polarisation factor* (dimensionless), which we have already introduced.**
  - $\mathcal{L}(\gamma)$ **is the so-called *Lorentz factor* (dimensionless), and contains all the experiment-specific geometrical factors arising from the δ-function integration.**
  - $\mathcal{A}_{\boldsymbol{\tau}}(\lambda,\gamma)$ **(dimensionless) is the *attenuation and extinction coefficient*, which account for the beam absorption and for dynamical effects.**
  - $\mathcal{F}_{inc}$ **is the incident time-integrated flux term (counts per square metre), which accounts for the strength of the incident beam and for the counting time.**

5 Structural solution from diffraction data

5.1 The phase problem

From eq. 4, we can see that **the structure factor is proportional to the Fourier transform of the charge density (or, more in general, scattering density) integrated over the unit cell**. By the elementary theory of the Fourier transform over a finite interval (extended to 3 dimensions) we can calculate the charge density given all the structure factors:

$$f(\mathbf{r}) = \frac{1}{r_0\, v_0} \sum_{\boldsymbol{\tau}} F(\boldsymbol{\tau}) e^{\boldsymbol{\tau}\cdot\mathbf{r}} \tag{27}$$

From eq. 27 follows that **if we were able to measure all the structure factors, we could reconstruct the charge density exactly**. Clearly, it is impossible to measure all the infinite nodes of the reciprocal space, but it can be shown that it would be sufficient to measure up to

a value of q_{max} to obtain a ***Fourier map*** with **resolution** $2\pi/q_{max}$ in *real space*. Therefore, the limited number of measured reflections does not pose an insurmountable problem to the reconstruction of the charge density

Direct reconstruction of the charge density is impossible, because only the *amplitudes* of the structure factors are known (through the term $|F|^2$ in the cross section), while the *phases* are unknown. Solving a crystal structure is therefore equivalent to *phasing* the reflections.

5.2 Methods to solve crystal structures

The Patterson method

Given that the scattering density cannot be determined without phasing the reflections, it is nonetheless possible to obtain some degree of information about it without any knowledge of the phases. Again, from eq 4, we obtain:

$$|F(\boldsymbol{q})|^2 = r_0^2 \iint_{unit\,cell} d\boldsymbol{r} d\boldsymbol{r}' f(\boldsymbol{r}) f(\boldsymbol{r}') e^{-i\boldsymbol{q}\cdot(\boldsymbol{r}-\boldsymbol{r}')} \tag{28}$$

With a change of variable (left as an exercise) and some manipulations we obtain:

$$\boxed{\frac{1}{r_0^2\, v_0} \sum_{\boldsymbol{\tau}} |F(\boldsymbol{\tau})|^2 e^{i\boldsymbol{\tau}\cdot\mathbf{r}} = \int_{unit\,cell} d\boldsymbol{r}' f(\boldsymbol{r}') f(\boldsymbol{r}+\boldsymbol{r}') = P(\mathbf{r})} \tag{29}$$

The function defined in eq. 29 is known as the ***Patterson function*** (or "Patterson" for the cognoscenti, from Lindo Patterson, 1934). One can perhaps recognise in eq. 29 that the Patterson is **the autocorrelation function of the scattering density**.

Important properties of the Patterson function for atomic-like scattering densities

- **Patterson functions are 3-dimensional functions defined within one unit cell, and are usually presented in the form of 2-dimensional "slices".**
- **Atomic-like scattering densities are *mostly zero*, except at the atomic positions. Therefore the Patterson function will be mostly zero as well, except at the *origin* ($\boldsymbol{r} = 0$) and *for values of $\boldsymbol{r}$ corresponding to vectors joining two atoms*. At these vectors, the Patterson function will have peaks.**
- **The height of the $\boldsymbol{r} = 0$ peak can be easily calculated (left as an exercise).**

Direct methods. If the scattering density was an arbitrary, complex function, solving *a priori* the phase problem would be impossible, since and infinite number of such functions would be compatible with a given set of $|F|^2$'s. However, *real* charge densities have three key properties that are extensively exploited by the so-called **direct methods** to "phase" the reflections, without any *a priori* knowledge of the crystal structure:

- Scattering densities are *real* functions (the imaginary anomalous term can be safely ignored, except near a resonance)..
- Charge densities are *positive* functions. Note that **Fermi lengths in neutron scattering can be positive and negative**, but special direct methods have been developed to deal with these problems.
- Scattering densities are *"atomic-like"*. In other words, if one has the correct phases, one should get *peaks* in the Fourier maps, whereas if the phases are wrong, the Fourier maps consists of oscillations throughout the unit cell.

Direct methods exploit a number of inequalities existing between terms of the Fourier series for positive-definite functions, to yield "probable" phase relations between sets of reflections (*pairs*, *triplet* and *quartets*) based on the ratios of their intensities. There are extensively exploited to solve single-crystal structures.

Structural "optimisation": least-square refinements. In general a certain degree of prior knowledge is always present before one attempts to solve a crystal structure, such as the stoichiometry and the number of formula units in the unit cell, sometimes the molecular connectivity etc. This can be incorporated in the solution strategy.

- If the information is fragmentary, one can incorporate it in the direct method approach, yielding more precise phase relations.

- If one is reasonably close of the solution, with only a few free parameters left to determine, it is possible to *minimise the agreement between observed and calculated squared structure factors $|F|^2$ as a function of the free parameters*. This is clearly a non-linear optimisation problem, and a number of strategies have been developed to solve it in a variety of cases.

Most problems in physical crystallography involve determining subtle structural variations from well-known and rather simple structural motifs. Therefore, structural optimisation is usually the method of choice for the structural condensed-matter physicist.

The Rietveld method All the structural solution techniques described above for single crystal diffraction have been adapted to powder diffraction, including the Patterson method and the direct methods. Clearly, one has to contend with the much greater **degeneracy** of powder data, which, as we have seen, are "compressed" into one dimension. Among the powder methods, one stands out by far, being almost ubiquitous in all applications: **the Rietveld methods** , discovered by the Dutch crystallographer Hugo Rietveld in 1969.

In the Rietveld method, one performs a nonlinear least-square fit *of the measured profile*, rather than of the $|F|^2$ as in the single-crystal methods. This could appear more complicated, since one has to fit the microstructural and instrumental parameters controlling peak broadening and the background at the same time, but has the great advantage of *accounting automatically for peak overlap*. This is illustrated in fig. 8.

6 Beyond the small-crystal approximation: dynamical diffraction and extinction

Up to this point, we have developed the diffraction formalism **strictly in the kinematic approximation**, i.e., **ignoring completely the interaction of the scattered beam with the crystal and the interference between the forward-scattered beam and the incident beam**. Taking this into account, in the so-called **full dynamical diffraction theory**, results in a series of rather unusual phenomena, Mainly observed in highly perfect crystals. **Extinction** is briefly outlined here below. For a full quantitative treatment, including that of **anomalous transmission (the Borrmann effect)**, see [5]

Extinction

- When the full dynamic theory is applied, the integrated intensity of each Bragg peak is always *lower* than expected from the kinematic theory — a phenomenon known as *extinction*. Although this reduction is not immediately apparent from the equations we presented, it

should be clear from the fact that *the most important consequence of the dynamical theory of scattering is to restore energy conservation*. We can think of this, intuitively, as if the scattered energy from each layer would be lost from the primary beam producing scattering from the next layer. Single crystal diffraction data *almost always* need to be corrected for extinction to yield realistic structure factors.

- In the full dynamic limit, *the integrated Bragg intensity is independent on the structure factor, and is instead proportional to the Darwin width*. Therefore, *diffraction data from large, highly perfect crystals are essentially useless to determine crystal structures*.

7 Bibliography

Stephen W. Lovesey, "Theory of neutron scattering from condensed matter" [1] is "the" textbook on the theory of neutron scattering and related matters.

G.L. Squires "Introduction to thermal neutron scattering" [2] is a classic introductory book.

E. H. Kisi "Applications of neutron powder diffraction" [3] is a more recent book on neutron diffraction, focussing on the powder method.

Warren, "X-ray diffraction" [4] is a rather old book with a very dated notation, but somehow I always find myself going back to it. Some of the explanations are very clear.

Authier, "Dynamical Theory of X-ray Diffraction" [5] is a very complete book on the dynamical theory of X-ray scattering. It has a good historical introduction and some simple explanations of the phenomena.

References

[1] Stephen W. Lovesey, "Theory of neutron scattering from condensed matter", Oxford Science Publications, Clarendon Press, Oxford (1984) — in 2 volumes.

[2] G.L. Squires "Introduction to thermal neutron scattering" Dover Publications, Cambridge, New York, 1978

[3] E. H. Kisi and C. J. Howard, "Applications of neutron powder diffraction", Oxford University Press, Oxford, New York, 2008.

[4] B.E. Warren, *X-ray diffraction* (Dover Publications, Inc., New York) 2nd Ed. 1990.

[5] André Authier, "Dynamical Theory of X-ray Diffraction", International Union of Crystallography, Oxford University Press (Oxford, New York), 2001.